Journal of
Synchrotron
Radiation

ISSN 1600-5775

Received 23 January 2014
Accepted 31 March 2014

A tunable wedge-shaped absorber for hard X-ray synchrotron applications

C. Krywka,[a,b]* M. Brix[b] and M. Müller[a]

[a]Helmholtz-Zentrum Geesthacht, Max-Planck-Strasse 1, D-21502 Geesthacht, Germany, and [b]Institute for Applied and Experimental Physics, University of Kiel, Leibnizstrasse 19, D-24098 Kiel, Germany. *E-mail: christina.krywka@hzg.de

The concept of a concave aluminium wedge-shaped absorber for hard X-ray synchrotron beamlines is presented. Unlike the commonly used absorber types (fixed-thickness absorber sheets or binary exchangers of individual fixed absorbers), this concept allows a compact system, controlled with a single linear positioner, and provides a wide attenuation range as well as a precise tunability over a large energy range. Data were recorded at the Nanofocus Endstation of the MINAXS beamline, PETRA III, Hamburg, Germany.

Keywords: absorber; attenuator; flux reduction; beamline instrumentation.

1. Introduction

X-ray absorbers at synchrotron radiation beamlines are primarily required to attenuate the direct beam in order to reduce flux density. Although a high flux density is generally desired and every effort is made to provide the highest brilliance, sometimes a temporary reduction of the incoming photon flux density is required. This can be the case when radiation-induced damage of the sample needs to be reduced in an X-ray diffraction experiment and if this cannot be performed by exposure time reduction alone. Attenuation is also essential for the alignment of many optical elements (X-ray mirrors, X-ray lenses, X-ray waveguides *etc.*) where detectors with limited count rates (CCD, proportional counter, live X-ray camera) are used to monitor changes while alignment parameters are tuned. Here, absorbers are not only required to prevent saturation, but more importantly to reduce the high incident flux in such a way that it fits into the used detector's limited dynamical range.

The absorber systems most commonly used at hard X-ray synchrotron beamlines contain a set of metal attenuators, each with a fixed thickness. The attenuators are inserted into the beam either one at a time or in a consecutive arrangement, usually using linear or rotating actuators. However, in order to obtain usable attenuation factors over several orders of magnitude within a wide photon energy range, a large quantity of individual attenuators is required, as will be shown in the following.

2. Absorption

For a flat sample of thickness d, the transmittance T, *i.e.* the ratio of the transmitted and the incident intensities, $I(d)$ and I_0, respectively, is determined by the linear absorption coefficient μ which in turn is related to the total absorption cross section $\sigma_{\rm abs}$,

$$T(d) = \frac{I(d)}{I_0} = \exp(-\mu d) = \exp\left[-\left(\frac{\rho_{\rm m} N_{\rm A}}{M}\right)\sigma_{\rm abs}\, d\right], \qquad (1)$$

where $\rho_{\rm m}$, $N_{\rm A}$ and M denote the mass density, Avogadro's number and molar mass, respectively (Als-Nielsen & McMorrow, 2001). At photon energies $E \ll 100$ keV the total absorption cross section basically equals the photoelectric cross section $\sigma_{\rm ph}$, *i.e.* $\sigma_{\rm abs} \simeq \sigma_{\rm ph}$ for most elements (Thompson & Vaughan, 2001). Unless in the vicinity of absorption edges, the cross section for the photoelectric effect is given by

$$\sigma_{\rm ph} \propto Z^5 E^{-3.5}, \qquad (2)$$

where Z is the atomic number (Grupen, 2010; Heitler, 1954). Consequently, in order to maintain the attenuation strength of a given absorber at an energy increased by 10%, its thickness needs to be increased by about 40%. The absorber system at a multi-energy beamline (like P03 MINAXS with a continuous energy range from 8 to 23 keV) must therefore be able to provide a wide range of absorber thicknesses, typically put into practice using a multi-stage absorber system with multiple attenuators inserted into the beam consecutively.

3. Multi-stage absorber exchangers

A typical absorber is a device assembled of m attenuators (usually non-identical) arranged consecutively and each of the attenuators can be moved into the beam or out of the beam individually. Such a system can generate 2^m attenuation strengths [more generally $(n+1)^m$ if each attenuator provides n different attenuation states].

A very useful demand is to have these 2^m attenuation strengths distributed *evenly* across all attenuation orders of magnitudes provided by the device. Having a constant number of attenuation factors per order of magnitude provides a precise tunability of the attenuation at every available energy or flux level. This condition is met only if the attenuator set contains thicknesses that increase in a geometric sequence, *i.e.* d, $2d$, 2^2d, $2^3d \ldots 2^{m-1}d$ (where d is the lowest thickness). At any given energy this system's dynamic range, DR, *i.e.* the ratio between the strongest and the weakest attenuation, is

$$\mathrm{DR} = \frac{T(d_{\rm min})}{T(d_{\rm max})} = \frac{T(d)}{T(2^m d - d)} = \exp[\mu d(2^m - 2)], \qquad (3)$$

where $d_{\rm max}$ is the sum of all attenuator thicknesses.

For example, to cover a dynamic range of three orders of magnitude with three attenuation steps in each of them, the absorber system must provide at least nine attenuation steps, hence $m \geq 4$ is required (such that $2^m \geq 9$). For a given absorber material and at a fixed energy [*e.g.* aluminium at 15 keV, μ = 1/497.608 µm (Gullikson, 2011)], using DR = 10^3 and m = 4, equation (3) yields $d = d_{\rm min}$ = 245.5 µm for the thinnest absorber thickness. The so-defined absorber set [d_1, d_2, d_3, d_4] = [245.5, 491, 982, 1964] µm has $d_{\rm max}$ = 3.7 mm, *i.e.* it has a thickness spread of $d_{\rm max} - d_{\rm min} \simeq$ 3.5 mm. At different energies, *e.g.* 10 or 20 keV, this value changes to 1 mm and 8 mm, respectively. So, despite the relatively small dynamic range demand, the attenuation requirements can only be satisfied for the entire energy range if the number of attenuators is increased and the minimal thickness decreased (*e.g.* $m \geq 7$ and d = 74 µm).

It must be noted that this finding is independent of the used absorber material. If a material with a higher Z is used, only the $d_{\rm max}$ and $d_{\rm min}$ values change, not the amount of required actuators. However, the resulting smaller value of $d_{\rm min}$ (*e.g.* 12.5 µm for silver at 15 keV) is difficult to handle and to obtain with a sufficiently low thickness tolerance. Also, absorption edges within the target energy span significantly reduce the system's usable energy range.

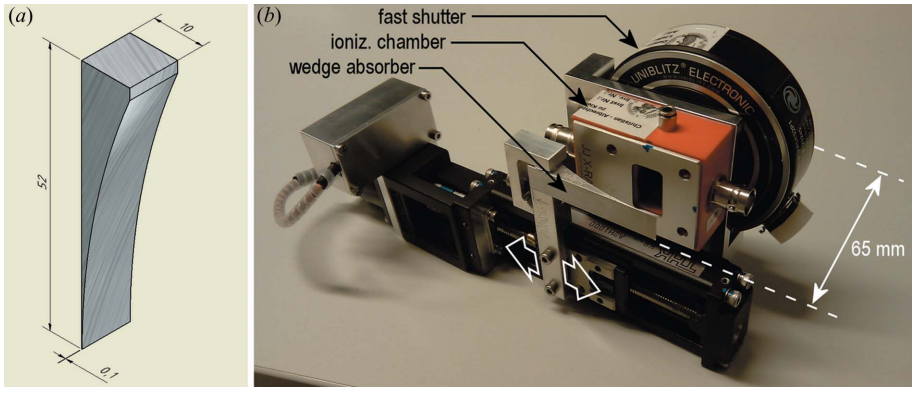

Figure 1
(*a*) Geometry of the concave wedge absorber, manufactured from aluminium (units of mm). (*b*) The wedge absorber is mounted on a single linear actuator and is part of a compact unit comprising the absorber, an ionization chamber and a fast shutter (installed at the P03 MINAXS beamline of PETRA III). The dimension of the unit is 65 mm along the beam direction.

4. Wedge absorber

Here, a compact absorber design is presented which is controlled by a single linear positioner and still provides a precisely tunable wide attenuation power range within a large energy span. A precisely machined concave wedge-shaped piece of aluminium is used as attenuator, which readily provides a continuous distribution of thicknesses and a high ratio between the thinnest and the thickest ends. Although (linear) wedge-shaped absorbers are being used as test objects for calibration of detector systems in medical X-ray radiography (Couture & Hildebolt, 2002) to match the contrast range of a radiographic imaging set-up with a given soft tissue sample (Hoshino *et al.*, 2013) or in differential phase-contrast imaging (Mukaide *et al.*, 2009), no such use for tunable X-ray attenuation is reported. This is mostly because at synchrotron beamlines typically a wide range of selectable attenuation must be maintained within a widely tunable energy range, which would require a long unhandy linear wedge. Because the absorber introduced here has a non-linear concave profile it can much better compensate the strong energy-related decrease of attenuation power [see equation (2)] than an equally sized linear wedge, thereby reducing space requirements. The geometry of the concave wedge absorber and a photograph of the entire unit are shown in Fig. 1.

Because this absorber requires only a single linear positioner, both the overall size of the system as well as its costs are rendered relatively small. At the Nanofocus Endstation of the MINAXS beamline of PETRA III (Krywka *et al.*, 2012, 2013), where this absorber is in continuous use, it is incorporated into a unit comprising the absorber, an ionization-chamber monitor and a fast shutter (see Fig. 1*b*). Yet the entire unit uses only 65 mm along the beam direction. Despite its small size, the absorber module generates a continuously tunable attenuation over more than six orders of magnitude for most of the energy range of the beamline (8–23 keV, see Fig. 2), by providing thicknesses between 0.1 and 10.1 mm along its concave curvature. The concave shape of the absorber is a circle segment (radius R = 130 mm) and the thickness at a specific distance x from the thin edge is

$$d(x) = d_0 + R - \left(R^2 - x^2\right)^{1/2}, \qquad (4)$$

where d_0 is the thickness at the thin edge. A circular profile is relatively easy to manufacture and the specific absorber used at MINAXS has a usable length of $x_{\rm max}$ = 50 mm (hence $d_{\rm max}$ = 10.1 mm) in order to maintain an attenuation range of three orders of magnitude at the maximum energy of $E_{\rm max}$ = 23 keV. At the same time it provides a low thickness increment at its thin end (*e.g.* 385 µm over the first 10 mm), which is important for precise tunability at low energies. If these specifications were to be met using a linear wedge, its length would be about 26 cm, *i.e.* five-fold larger.

At the MINAXS beamline a compact linear positioner with gear reduction and a small stepper motor are used to move the absorber to the desired position, which, despite the low cost of this arrangement, can be performed with single-micrometer reproducibility. If required, the stepper motor can be operated at a speed which allows setting the maximal attenuation within ~1 s, *i.e.* sufficiently fast to respond to a strong beam inadvertently hitting the detector. As only little mass is

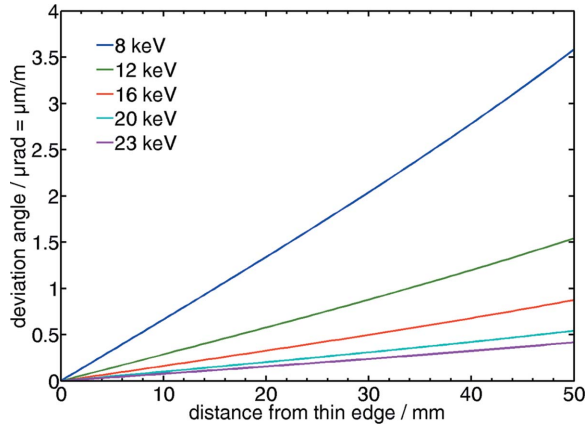

Figure 2
Calculated beam deviation angle due to refraction of the incident beam at the curved surface of the wedge absorber. The calculation was performed for selected energies, covering the entire energy range of the beamline.

moved, a piezo positioner may as well be used instead, allowing for even shorter move times. In order to reduce thickness deviations due to the surface roughness of a machined part (10 µm order), which of course are relatively largest at the thin end of the wedge, its face sides were manually polished and lapped to achieve even mirror-like surfaces. The wedge was manufactured from high-purity aluminium in order to avoid fluorescent emission from the compounds usually found in the common aluminium alloys (Mg, Mn, Cu, Zn). The highest emission line of aluminium ($K\beta1$) is at 1.557 keV, so the emitted fluorescence can be neglected as it is effectively shielded after 10 cm of air (Thompson & Vaughan, 2001) and so the device can be conveniently operated close to the sample position.

Owing to the curvature of the absorber, the X-ray beam penetrates the metal interface at non-orthogonal incidence angles, which is why the refractive effect of the attenuator needs to be taken into account. Assuming a normal incidence onto the flat face of the wedge, the curved interface between aluminium (refractive index n_1) and air ($n_2 = 1$) is intercepted at an angle α_1 (where $\alpha_1 = 0$ corresponds to normal incidence). The wavefront will be refracted at the angle α_2 defined by Snell's law,

$$\frac{\sin\alpha_1}{\sin\alpha_2} = \frac{n_2}{n_1} = \frac{1}{1-\delta+i\beta}, \tag{5}$$

where δ and β denote the wavelength-dependent dispersion and absorption, respectively (Als-Nielsen & McMorrow, 2001). For X-ray photon energies from 8 to 23 keV and aluminium, no absorption-edge effects need to be taken into consideration. The effective beam deviation angle due to refraction is then

$$\alpha_1 - \alpha_2 = \arcsin(x/R) - \arcsin[(x/R)(1-\delta)], \tag{6}$$

and is shown for different photon energies in Fig. 2. Obviously the refraction angle is of single microradian order, *i.e.* the beam center is shifted only by single micrometer per meter beam path. This is in most cases negligible especially as the absorber can be installed close upstream of the sample position and beam orbit instabilities have usually a greater impact at beamlines. This is valid even for beamlines with a nanofocused beam (such at the Nanofocus Endstation of MINAXS P03, where the beam size is 250 nm × 350 nm). Here absorbers are placed upstream of the nanofocusing optics, in order not to compromise the short working distance, and therefore the miniscule variation of the beam direction introduced by the absorber is again negligible.

For most accurate measurements, the variation of the absorber thickness across the beam profile may be detrimental. This is only a small effect for any microfocused beam: at MINAXS the beam size at the absorber is about 100 µm and so the intensity variation over the beam profile is less than 1% with the given absorber profile. A millimeter-sized beam, however, will experience stronger modulations unless the impact is reduced by using a larger value of R. Alternatively, two wedge absorbers could be used in an opposite motion geometry to compensate for the asymmetric attenuation without extending the length of the wedge absorber(s). Such a set-up would also compensate the previously mentioned beam refraction effect.

5. Experimental data

To verify the calculated transmission profiles, the intensity transmitted through the absorber was recorded as a function of the absorber thickness (*i.e.* position of the beam on the absorber) at the Nanofocus Endstation of the MINAXS beamline, at a photon energy of 12.8 keV (see Fig. 1). The incident intensity I_0 was measured using the ionization chamber (JJ-X-ray) situated directly in front of the absorber. The attenuated intensity $I(d)$ was measured behind the absorber using two different detector types in order to provide the dynamic range required to cover the anticipated six orders of magnitude of attenuation. The measured transmittance is shown in Fig. 3 along with calculated data. A calibrated PIN-diode (Canberra CAM-300 AB) and a NaI(Tl)-scintillation counter (Cyberstar) were used in the 0.1–4.0 mm and 3.6–5.2 mm thickness ranges, respectively. At 3.6 mm and at 5.2 mm the noise levels for the PIN-diode and the scintillation detector, respectively, were reached, *i.e.* the output signal no longer decreased with stronger attenuation. A small portion of the data around 0.6 mm is omitted due to corrupted data. Linear extrapolations were used to intercalibrate the intensity scales of the two data sets. An excellent accordance of the experimental and the calculated data is evident over four orders of magnitude, below which a distinct deviation is visible indicating a non-uniform thickness excess in the corresponding portion of the absorber. The thickness excess was confirmed experimentally and could be deduced to a misalignment of the machining tool. Even though this could have been encountered by a more careful tool alignment, such misalignment usually does not compromise the usability of the absorber, whose most important feature is the precise tunability over a wide range of absorption power. If precise absolute attenuation values are indeed of relevance, a calibration curve can be recorded during initial commissioning of the absorber and modeled in order to obtain an analytic attenuation profile.

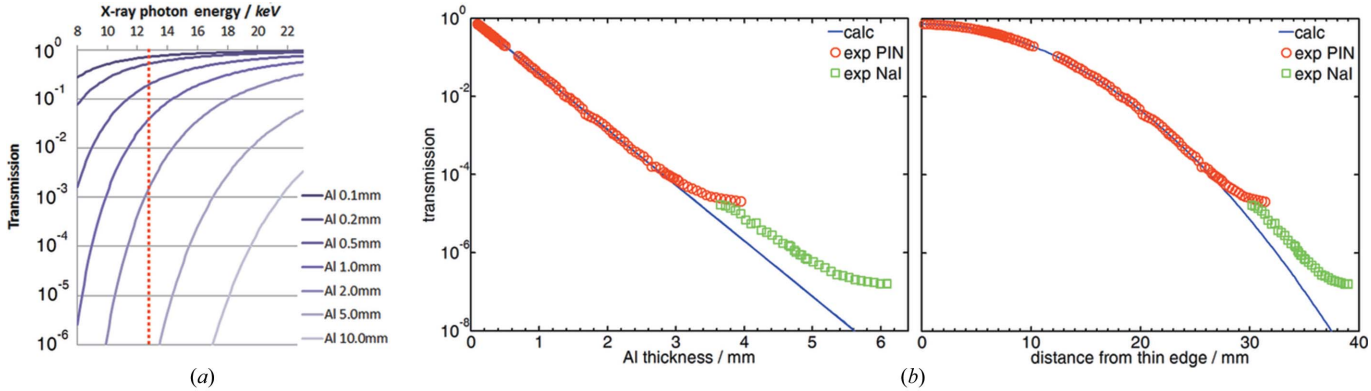

(*a*) (*b*)

Figure 3
(*a*) Calculated transmittance for selected absorber thicknesses within the beamline's energy range (8–23 keV). The vertical dotted line represents the energy (12.8 keV) at which the high-resolution transmittance data were recorded as a function of absorber thickness and which is shown in the two panels of (*b*).

6. Conclusion

A new type of absorber for use at hard X-ray synchrotron beamlines was presented based on a concave wedge-shaped aluminium part. It allows a very compact and economical assembly and can be controlled with a single linear positioner. Despite its simplicity, it provides an attenuation range of more than six orders of magnitude for most of the energy range of the P03 MINAXS beamline (8–23 keV) at the PETRA III synchrotron source, yet it is precisely tunable within each order of magnitude. It was pointed out that these specifications could not have been met using an equally sized linear wedge absorber and that using a conventional absorber exchanger would require a significant amount of independent positioners. It was shown that, despite the low manufacturing effort of the wedge absorber, an excellent accordance of experimental and calculated attenuation powers can be achieved for four orders of magnitude. It was also demonstrated that issues resulting from the absorber's uneven geometry (beam deviation due to refraction and beam profile variation due to absorption) can be considered negligible in most cases and that they can be effectively encountered for those very accurate measurements in which they may be detrimental.

The Nanofocus Endstation of the MINAXS (P03) beamline was equipped through financial support by the German Federal Ministry of Education and Research (BMBF projects 05KS7FK3 and 05K10FK3), which is greatly acknowledged. We thank the P03 beamline team for provision of the beam to the Nanofocus Endstation.

References

Als-Nielsen, J. & McMorrow, D. (2001). *Elements of Modern X-ray Physics*. New York: Wiley.
Couture, R. A. & Hildebolt, C. F. (2002). *Dentomaxillofacial Radiol.* **31**, 56–62.
Grupen, C. (2010). *Introduction to Radiation Protection: Practical Knowledge for Handling Radioactive Sources*, p. 44. Berlin/Heidelberg: Springer.
Gullikson, E. (2011). *CXRO X-ray Interactions With Matter*, http://henke.lbl.gov/optical_constants/.
Heitler, W. (1954). *The Quantum Theory of Radiation*, 3rd ed., p. 204. Oxford University Press.
Hoshino, M., Uesugi, K., Sera, T. & Yagi, N. (2013). *J. Instrum.* **8**, P07018.
Krywka, C., Keckes, J., Storm, S., Buffet, A., Roth, S., Döhrmann, R. & Müller, M. (2013). *J. Phys. Conf. Ser.* **425**, 072021.
Krywka, C., Neubauer, H., Priebe, M., Salditt, T., Keckes, J., Buffet, A., Roth, S. V., Doehrmann, R. & Mueller, M. (2012). *J. Appl. Cryst.* **45**, 85–92.
Mukaide, T., Takada, K., Watanabe, M., Noma, T. & Iida, A. (2009). *Rev. Sci. Instrum.* **80**, 033707.
Thompson, A. C. & Vaughan, D. (2001). *X-ray Data Booklet*, p. 3–2. Lawrence Berkeley National Laboratory, University of California Berkeley, CA, USA.